Lund-MPh-09/01
LU-TP 09-15

# Parton correlations in high energy proton-proton scattering

Jonas Nordström

Master's thesis
Lunds Tekniska Högskola
Supervisor: Leif Lönnblad
Examiner: Ragnar Bengtsson

Juni, 2009

## Abstract

In this thesis we will use the Monte Carlo(MC) event generator DIPSY to study correlations in proton-proton scattering. DIPSY uses a modified version of the Mueller dipole model to dynamically create the wave function of a proton, or at least a very simple approximation thereof.

We will look at the correlation between the inverse dipole sizes and the number of dipoles, or the number of subscatterings, to see the effects screening. We will also look at some correlation that may give a dynamical explanation to some of the assumptions made in the multiple interaction model implemented in the PYTHIA MC. These assumptions include, the distribution of the number of subscatterings both at fixed impact parameter and as an average aver all impact parameters, and the shape of the overlap (of the wave functions) of two colliding protons.

The DIPSY program is still under development, and the results presented here should be considered preliminary.

# Acknowledgments

I would like to thank my supervisor Leif Lönnblad, and my unofficial co-supervisor Gösta Gustafson, for their efforts in explaining the mystery that is dipoles. A special thanks to Christoffer Flensburg for the time spent, helping me to understand DIPSY.

I also thank Torbjörn Sjöstrand for some valuable discussions.

Jonas Nordström

# Contents

# Introduction

Understanding proton-proton ($pp$) scattering is an important topic these days when the LHC is about to start (hopefully). Protons consists of partons, and when two protons collide at high energies it is in fact the partons that interact. Since there are several partons in each proton it is not unlikely that there will be several parton subscatterings in a single $pp$-scattering.

At small distances perturbative quantum chromo dynamics (pQCD) tells us how the partons interact, however, the distribution of the partons inside the proton can not be calculated, as they depend on non-perturbative, highly non-linear effects at small energy scales. Also at the energy scales where pQCD is valid we expect there to be some non-linear effects. These are hard to calculate analytically, we therefore use a Monte Carlo event generator (MC) to simulate scatterings in this region.

The parton-parton cross section calculated with pQCD turns out to be infinite, it behaves as a Rutherford scattering. Therefore, we introduce a cutoff that limits the chance for soft scatterings, i.e. scatterings with a small transfer of momentum. This cutoff is related to the distance at which the color field of a parton vanishes due to screening from other color charges.

The PYTHIA MC, [26], is very successful in simulating the final states of $pp$-scatterings. However it makes a number of assumptions in order to describe experimental data, we present some of these assumptions. The first is the distribution in coordinate-space of the partons inside a proton, the parton density is assumed to be given by two super positioned Gaussian distributions, this assumption is not absolute, but a simple Gaussian will not do the job, so the proton needs a core of some sort. The number of subcollisions is then proportional to the overlap of the two protons. Another assumption is that at fixed impact parameter (the distance between the centers of the two incoming protons) the number of subscatterings is given by a Poisson distribution. Combining these two assumptions, the number of subscatterings integrated over all impact parameters behave as a geometric distribution. Screening is also assumed in PYTHIA and helps to increase the average transverse momentum, the momentum in the directions perpendicular to the collision axis, in the subscatterings. This is because it cuts down on the soft subscatterings.

One way to study the increase in transverse momentum is to view it as a function of the charged multiplicity, the number of charged particles created in the collision. In experiments this is a increasing function. In order for PYTHIA to fit to this data, it requires maximal color reconnection in the hadronization (the creation of the charged particles) using the (Lund) string model. There is, however, no real theoretical basis for this maximal color reconnection.

DIPSY, [12] ([10, 11]), is a new MC based on a modified, [4, 5, 6, 7], version of the Mueller dipole model, [21, 22, 23]. Unlike previous MCs based on the Mueller dipole model, which could only be used to calculate inclusive properties this will be able to produce exclusive final states, when it is completed.

The Mueller dipole model, views a proton as consisting of color dipoles given in transverse coordinate-space. As we accelerate the proton the dipoles will emit gluons as bremsstrahlung, these gluons make up new dipoles, and we get a cascade of dipoles. Since the dipoles, and therefore the gluons from which they are built are given in coordinate space we will get a method for constructing the parton distribution in the protons. If we can also keep track of the gluons transverse momenta we will be able to produce the final states.

The first MC bases on the dipole model was [25], it suffered from severe numerical problems, due to the fact that far to many small dipoles was created. These slowed the program down while not giving any contribution to the cross section. In an other MC using the dipole model, [4], there was introduced an energy conservation rule in the emission process, that slows down the rapid growth of the small dipoles.

This is also the basis of DIPSY, where we create the parton distribution dynamically. This, we hope, will produce results that may explain why the assumption made in PHYTIA works. At the moment the method for keeping track of the momenta is not ready and thus we will not be able to test the increase in average transverse momentum directly.

The thesis start with a chapter on the theory of partons. We will describe two method for estimating the parton distributions given in fraction of the protons momentum, called, DGLAP and BFKL. We will give a simplified method for calculating the emission and interaction probability in the Mueller dipole model, and then we give some further additions made to this model in DIPSY.

Then there is a brief chapter of the implementation of these additional assumption in DIPSY, without going into programming details.

We will also present some results, we find that there is in essence a Poisson distribution for fixed impact parameter, and integrating over all impact parameters does in fact give a geometric distribution. We will see some indications that DIPSY predicts an increase in the average transverse momentum as a function of the charged multiplicity.

# Chapter 1

# Theory

Protons are bound states of partons (quarks and gluons). To be able to predict what happens in a proton-proton ($pp$) scattering at high energies we therefore need to know both how the partons interact and the distribution of the partons. In this chapter we present the standard way of describing interactions and parton distributions, we also present the dipole formalism.

## 1.1 Particle kinematics

The material in this section is independent of partons and protons, it is, however, very useful when studying these objects.

### 1.1.1 Light-Cone system

In high energy scattering, it turns out, that the best way of representing the momentum is in the light-cone (LC) system, where we divide the momentum in a part along the axis of movement, in our case the $z$-axis, and one part in the perpendicular plane, the $xy$-plane.

We start with a given four-momentum $p^\mu = (E, -p_x, -p_y, -p_z)$ and coordinate $x^\mu = (t, -x, -y, -z)$. From this we define the LC-coordinate and momentum by

$$\begin{aligned} p_\pm &= E \pm p_z, \quad \mathbf{p} = (p_x, p_y) \\ x_\pm &= t \pm z, \quad \mathbf{x} = (x, y)\,, \end{aligned}$$

where we also set $p = |\mathbf{p}|$ and $x = |\mathbf{x}|$.[1]

Using the LC-coordinates we define the rapidity[2] as

$$y = \frac{1}{2} \ln\left(\frac{p_-}{p_+}\right).$$

The rapidity is linear under a boost, i.e. for a boost $\beta$ in the $z$-direction we have $y' = y + f(\beta)$, so that $dy = dy'$ is Lorentz invariant.

For a massless on-shell particle we have the relation

$$0 = m^2 = p^\mu p_\mu = p_- p_+ - p^2.$$

[1]When we use three-dimensional coordinates and momenta, we shall denote them by $\bar{p} = (p_x, p_y, p_z)$ and $\bar{x} = (x, y, z)$.

[2]Usually the rapidity is defined with the opposite sign.

Thus we find that we can express the rapidity as

$$y = \frac{1}{2}\ln\left(\left(\frac{p}{p_+}\right)^2\right) = \ln\left(\frac{p}{p_+}\right),$$

or equivalently $p_+ = pe^{-y}$.

### 1.1.2 Mandelstam variables

In a particle scatterings the most important kinematic variables are the center-of-mass (CM) energy and the transfered momentum. For a $p_1 + p_2 \rightarrow p_3 + p_4$ particle scattering we define the three Mandelstam variables

$$\begin{aligned}
s &= (p_1^\mu + p_2^\mu)^2 = (p_3^\mu + p_4^\mu)^2 \\
t &= (p_1^\mu - p_3^\mu)^2 \\
u &= (p_1^\mu - p_4^\mu)^2 .
\end{aligned}$$

Here $s$ is the square of the CM energy and $t$ is the square of the momentum transfer. If the particles are massless, and we look in the CM-frame, then they have LC-momenta

$$\begin{aligned}
(p_{1+}, \mathbf{p}_1, p_{1-}) &= (\sqrt{s}, (0,0), 0) \\
(p_{2+}, \mathbf{p}_2, p_{2-}) &= (0, (0,0), \sqrt{s})
\end{aligned}$$

before the collision and

$$\begin{aligned}
(p_{3+}, \mathbf{p}_3, p_{3-}) &= \frac{\sqrt{s}}{2}(1+\cos(\theta), (0, \sin(\theta)), 1-\cos(\theta)) \\
(p_{4+}, \mathbf{p}_4, p_{4-}) &= \frac{\sqrt{s}}{2}(1-\cos(\theta), (0, -\sin(\theta)), 1+\cos(\theta))
\end{aligned}$$

after the collision. We have

$$-t = p_{1+}p_{3-} + p_{1-}p_{3+} - \mathbf{p}_1 \cdot \mathbf{p}_3 = s\frac{1-\cos(\theta)}{2} = s\sin^2(\theta/2),$$

and

$$p^2 = \frac{s}{4}\sin^2(\theta).$$

We see that for small $\theta$ we have $-t \approx s\frac{\theta^2}{4} \approx p^2$ and therefore,

$$\frac{d\sigma}{d\Omega} \propto \frac{d\sigma}{dt} \propto \frac{d\sigma}{dp^2}$$

i.e. the differential cross section may be given in $p^2$.

The scatterings that we will look at are high energy scatterings between gluons. The differential cross section for this type of scattering is

$$\frac{d\sigma}{dp^2} \propto \frac{1}{p^4} \propto \frac{1}{\sin^4(\theta/2)},$$

which is the cross section for Rutherford scattering, elastic scattering between charged point-like particles. This implies that the biggest contribution to the cross section comes from the low $p$ transfer.

### 1.1.3 Bremsstrahlung

As the protons are accelerated they emit bremsstrahlung, this will increase the number of gluons in the proton. The rate of this emission can be calculate by simple methods, based on [18]. We consider a stationary observer, placed at $(\mathbf{r}, 0)$, measuring the gluons emitted by a color charge rapidly moving in the $z$-direction, and passing trough $\bar{r} = 0$ at $t = 0$. By the nature of the color force it will behave, approximately, as an electric field. The energy intensity of the emitted gluons for the Lorentz-contracted field is, as is shown in the appendix,

$$I(t) \propto \alpha_s \frac{1}{r^2} \delta(t) \,.$$

Since the intensity is a $\delta$-function in time it must be constant in frequency. Thus the energy intensity, given by frequency, is constant, and the number density per frequency, i.e. the number of gluons with energy $\omega$, is given by

$$dn \propto \alpha_s \frac{d^2\mathbf{r}}{r^2} \frac{d\omega}{\omega} = \alpha_s \frac{d^2\mathbf{q}}{q^2} \frac{d\omega}{\omega}.$$

If we set $x = \frac{\omega}{P_{proton}}$, i.e. $x$ is the fraction of the protons momentum carried by a gluon with energy $\omega$, and the rapidity $Y = \ln(1/x)$ then $\frac{d\omega}{\omega} = dY$ so the number density for an emission is

$$dn \propto \alpha_s \frac{d^2\mathbf{q}}{q^2} dY \propto \alpha_s \frac{dq^2}{q^2} dY.$$

We find that if there is a large rapidity range we will get a lot of emitted gluons.

## 1.2 Standard parton model

As stated before, protons consist of parton. In first approximation, they consist of three valence quarks. There are, however, also a lot of virtual quarks and gluons. Deeply inelastic scattering (DIS) was used to probe the structure of protons before the invention of QCD. We will describe DIS to introduce the notation of the standard parton model.

### 1.2.1 Deeply inelastic scattering

We have an electron with incoming momentum, $k^\mu$, and outgoing momentum, $k'^\mu$, the change in momentum goes to a photon with momentum, $q^\mu$, and virtuality, $Q^2 = -q^\mu q_\mu$, this measures the momentum transfer of the electron-proton($ep$) scattering. The photon interacts with a quark in the proton. The proton has positive LC-momentum, $P_+$, and the quark has momentum, $p_+ = xP_+$. At high energy, the only significant contribution to the momentum comes from the positive LC-momentum and thus we may write $p^\mu \approx xP^\mu$. We calculate $(p^\mu + q^\mu)^2$ and find

$$0 = (p^\mu + q^\mu)^2 = (xP^\mu + q^\mu)^2 = 2xP^\mu q_\mu - Q^2,$$

$(p^\mu + q^\mu)^2 = 0$ since it is the square of the new four momentum of the quark, which is considered to have negligible mass. Thus the fractional momentum of the quark can be measured as $x = \frac{Q^2}{2P^\mu q_\mu}$.

We define the parton density function (PDF), $f_i\left(x, Q^2\right)$, that gives the number of partons of a certain type, carrying a fraction, $x$, of the protons momentum/energy when measured by a photon of virtuality $Q^2$. If one measures the momentum carried by the quarks one finds that

$$P_{quarks} = \sum_q \int x f_q(x, Q^2) dx < P_{proton}.$$

Thus there are some electrically uncharged particles inside the proton. These are the gluons. From this we can indirectly measure the PDFs of the gluons. As it turns out the $f_i$:s are in fact functions of $Q^2$, at higher scales the PDF:s are peaked for smaller $x$. Gluons are massless bosons that have two color indices, they have a color and an anti-color. This in contrast to quarks which are massive fermions that only have one color index, a color for quarks and an anti-color for anti-quarks.

We use the cross section for an electron-quark scattering,

$$\frac{d\hat{\sigma}_{eq}}{dQ^2} = \frac{\pi\alpha^2}{Q^4} e_q^2,$$

which is calculatable in QED, and the PDF:s to get the *ep*-cross section

$$\frac{d\sigma_{ep}}{dQ^2} = \sum_q \int \frac{d\hat{\sigma}_{eq}(x)}{dQ^2} f_q\left(x, Q^2\right) dx.$$

### 1.2.2 *pp*-scattering

For two colliding protons, $Q^2 = -\hat{t} \approx p^2$ is the momentum transfer between the partons involved in the scattering. We get the following expression for the subscattering cross section

$$\frac{d\sigma_{sub}}{dp^2} = \sum_{i,j} \int\int f_{i,1}\left(x_1, p^2\right) f_{j,2}\left(x_2, p^2\right) \frac{d\hat{\sigma}}{dp^2}\left(x_1 x_2 s\right) dx_1 dx_2.$$

Since the parton-parton interaction is just Rutherford scattering, $\frac{d\hat{\sigma}}{p^2} \propto \frac{1}{p^4}$, the cross section diverges, which is clearly un-physical. Thus we introduce a cutoff, such that very small momentum transfers are suppressed. Even with this cutoff we find that eventually the subscattering cross section, $\sigma_{sub}$, is larger that the total cross section, $\sigma_{tot}$. By the total cross section we mean the non-diffractive inelastic one, i.e. the cross section for at least one hard subscattering. The interpretation of $\sigma_{sub} > \sigma_{tot}$ is that we have more than one subscattering and that the average number of subscatterings is given by

$$\langle n \rangle = \frac{\sigma_{sub}}{\sigma_{tot}}.$$

A small transfer of momentum is related to an interaction over a large distance, so the cutoff makes it harder for the partons to interact over large distances. Since protons are color singlets there must be a distance where the color field of a parton is screened by the other partons.

In PYTHIA, [26], rather than using a sharp cutoff $p_{min}$, a regularization scale is introduced to make the cross section finite,

$$\frac{d\hat{\sigma}}{dp^2} \propto \frac{\alpha_s^2(p^2)}{p^4} \rightarrow \frac{\alpha_s^2(p^2 + p_0^2)}{\left(p^2 + p_0^2\right)^2}.$$

Experiments give a value, $p_0 \approx 2$ GeV, for the cutoff.

### 1.2.3 Multiple interactions and color reconnections

As in, [16], we let $P_1$ and $P_2$ be the probabilities for one or two subscatterings, respectively. Then they have cross sections $\sigma_1 = P_1\sigma_{tot}$ and $\sigma_2 = P_2\sigma_{tot}$, respectively. If all subscatterings where uncorrelated, then we would have $P_2 = \frac{1}{2}P_1^2$, and

$$\sigma_2 = \frac{1}{2}\frac{\sigma_1^2}{\sigma_{tot}}.$$

In experiments it has been found that this is not true, and we have to replace $\sigma_{tot}$ by something smaller. This tells us that if there is one hard subscattering, there is a higher probability of another than if they had been uncorrelated. We interprets this as, head-on collisions gives a large probability for interaction while collisions over large distances are unlikely.

This is incorporated in the multiple interaction model in PYTHIA, [26]. The model relies on some specific assumptions, as follows.

The assumption on the protons, is that the parton densities of the protons are given by a double Gaussian, i.e.

$$\frac{\rho\left(\bar{r}\right)}{d^3\bar{r}} = \frac{\beta}{a_1^3}e^{-\frac{|\bar{r}|^2}{a_1^2}} + \frac{1-\beta}{a_2^3}e^{-\frac{|\bar{r}|^2}{a_2^2}},$$

where $\beta = 0.5$ and the quotient of $a_1$ and $a_2$ are chosen to fit experiments. The exact form of these distributions is not so important but we need a higher central density since we expect there to be alot of activity in a head-on collision.

The probability for an interaction, and in turn the average number of subscatterings, $< \tilde{n} >$, where $\tilde{n} = 0$ is allowed, at a given impact parameter, $b$, is proportional to the overlap, $\mathcal{O}\left(b\right)$, of the parton densities of the protons.

Also at a given impact parameter the number of subscatterings is assumed to be given by a Poisson distribution i.e.

$$P_{\tilde{n}}(b) = \frac{\langle\tilde{n}(b)\rangle^{\tilde{n}}}{\tilde{n}!}e^{-\langle\tilde{n}(b)\rangle}.$$

We are interested in the scatterings where there is at least one interaction, thus we need to rescale the distributions so that

$$P_n(b) = \frac{\langle\tilde{n}(b)\rangle^{n}}{n!}\frac{e^{-\langle\tilde{n}(b)\rangle}}{1-e^{-\langle\tilde{n}(b)\rangle}},$$

where $n$ is the number of interactions, where there is at least one interaction. The relation between $\langle n(b)\rangle$ and $\langle\tilde{n}(b)\rangle$ is

$$\begin{aligned}
\langle n(b)\rangle &= \sum_{n=1}^{\infty} nP_n(b) \\
&= \frac{e^{-\langle\tilde{n}(b)\rangle}}{1-e^{-\langle\tilde{n}(b)\rangle}}\langle\tilde{n}(b)\rangle\sum_{n=1}^{\infty}\frac{\langle\tilde{n}(b)\rangle^{n-1}}{(n-1)!} \\
&= \frac{\langle\tilde{n}(b)\rangle}{1-e^{-\langle\tilde{n}(b)\rangle}}.
\end{aligned}$$

It is shown in [14] that $P_{\tilde{n}} = \frac{\int P_{\tilde{n}}(b) d^2\mathbf{b}}{\sigma_{tot}}$ is approximately given by a geometric distribution, i.e.

$$P_{\tilde{n}} = (1-p)^{\tilde{n}} p,$$

where $\tilde{n} = 0, 1, \ldots$ and $\langle \tilde{n} \rangle = \frac{1-p}{p}$.

The gluons from an interaction are color-connected into strings. Every string consist of several string pieces, where every string piece consists of a color and a matching anti-color. Every piece has a mass/energy, $m_j^2$, that can be radiated off into hadrons. This mass/energy is given by $m^2 = (p_1^\mu + p_2^\mu)^2$, where $p_i^\mu$, $i = 1, 2$, are the four-momenta of the gluons at the endpoints of the string piece. When the string breaks by the creation of quark-anti-quark pairs, the number of charged particles created is, see [3],

$$N_{ch} \propto \sum_{j=1}^{N} \ln \left( m_j^2 / m_0^2 \right),$$

where $m_0$ is some constant, this formula only holds if all $m_j \leq m_0$, since no string piece can give a negative contribution. The transverse momentum of a created particle consists of two parts. The first part is given by a Gaussian distribution, [2]. This part gives an average $p_0$ to the average transverse momentum $\langle p \rangle$. The other part comes from the transverse momenta of the gluons. This part is predominantly given to the quarks that are produced later on with a low transverse momentum from the first part. Thus this will contribute with $\sum_n p_n / N_{ch}$ to the average transverse momentum, where the sum runs over all gluons. Therefore, the average transverse momentum is

$$\langle p \rangle = p_0 + \sum_n p_n / N_{ch}.$$

In [26], the authors found that if they assumed that each hard subscattering produced a new set of strings the increase of the function $\langle p \rangle (N_{ch})$ would not be large enough to fit experiments. At least some of the subscatterings would need to give strings that are not stretched far in the $z$-direction, and then must be considered as perturbations on the large string from the first subscattering.

If we do that, then there will be fewer string, also the total string length will be less. Therefore we produce fewer charged particles and there will be fewer particles that have to share the transverse momenta of the gluons.

It has been suggested by, [19], that the screening depends on the number of subscattering, called enhanced screening, and that this may give an increase in the $\langle p \rangle (N_{ch})$ function. Enhanced screening is implemented in PYTHIA by replacing $p_0^2$ by $np_0^2$, where $n$ is the number of subscatterings. The enhanced screening has been tested in [8]. With this implementation the enhanced screening could account for about a third of increase.

### 1.2.4 DGLAP- and BFKL-equations

In this section we give a simple derivation of the so called DGLAP-equation, based on [15]. The same reference is also used to derive of the behavior of gluons at small $x$, the behavior that can also be obtained from the so called BFKL-equation. The results can be obtained by more rigorous methods, see [13].

From the PDF we define the quark and the gluon functions $F(x,Q^2) = xf_q(x,Q^2)$ and $G(x,Q^2) = xf_g(x,Q^2)$. We want to calculate the approximate behavior of these functions.

We start with the quark function. In DIS, a photon with virtuality, $Q^2$, hits a quark with initial momentum $p_+ = x_0 P_+$ where $P^\mu$ is the momentum of the proton. Before the photon hits it is possible that the quark has sent out gluons and lowered its fractional momentum to $xP_+$. A photon of virtuality, $Q^2$, can only measure the decrease in the quark's momentum if the gluons live so long that they do not recombine with the quark during the time the photon exist. Since the life time of the photon is approximately the inverse of the virtuality we only include the gluon emission where $q_i^2 < Q^2$.

In a process where a quark sends out $n$ gluons, we study all chains such that $x = x_0 \prod_{i=0}^{n} z_i$ where each gluon takes a fraction $(1 - z_i)$ of the quarks momentum. Each emission has an approximate probability $dP \approx \frac{4\alpha_s}{3\pi}\frac{dz_i}{1-z_i}\frac{dq_i^2}{q_i^2}$. Of course, the first emitted gluon must have the lowest $q_i^2$ since it must have the longest life time prior to the quark being hit by the photon so we order the gluons according to

$$q_1^2 < q_2^2 < \ldots < q_n^2 < Q^2.$$

Thus the probability that the momentum $xP$ is reached in $n$ steps is

$$P_n\big(x,Q^2\big) \approx \prod_{j=1}^{n} \int_{q_{j-1}^2}^{Q^2} dq_j^2 \int_{x/x_0}^{1} dz_j \left[\delta\left(x - x_0 \prod_{j=1}^{n} z_j\right) \theta\left(Q^2 - q_n^2\right) S\left(q_j^2, q_{j-1}^2\right) \frac{4\alpha_s}{3\pi q_j^2\left(1 - z_j\right)}\right]$$

where $q_0 \approx 1$ GeV and $S\left(q_j^2, q_{j-1}^2\right)$ is a Sudakov factor to take into account the fact that there is only one quark that hits the probe and, therefore, there can be no gluon emissions with $q_i^2 \in \left(q_j^2, q_{j-1}^2\right)$. The quark density function is given by the probability that $x$ is reach in any number of steps i.e.

$$F\big(x,Q^2\big) \approx \sum_{n=0}^{\infty} P_n\big(x,Q^2\big)\,.$$

By differentiating this with respect to $Q^2$ we obtain the DGLAP-equation

$$\frac{\partial F(x,Q^2)}{\partial \ln(Q^2)} = \frac{4\alpha_s}{3\pi}\int dz dx' \hat{P}\left(z\right) F\left(x',Q^2\right)\delta\left(x - zx'\right),$$

where $\hat{P}$ replaces $\frac{1}{1-z}$. Thus if we know $F(x,Q_0^2)$ for all $x$ at some $Q_0^2$ we can calculate $F(x,Q^2)$ for all $Q^2$ where the DGLAP-equation is valid.

If we instead study $G(x,Q^2)$, we assume that we have some probe with virtuality, $Q^2$, that can interact with gluons, and measure the gluon function. We start with a gluon with fractional momentum $x_0$. This gluon will emit gluons and thus lower its fractional momentum to $x$, before interacting with the probe. We call the gluon that interacts with the probe the ladder gluon.

In a $g \to gg$ emission one of the gluons will retain the spin and most of the momentum of the parent gluon. In the case where it is the ladder gluon, that retains the parent characteristics the emission has a approximate probability

$$\frac{3\alpha_s}{\pi}\frac{dz_i}{1 - z_i}\frac{dq_i^2}{q_i^2}\theta\left(q_i - q_{i-1}\right) S\left(q_j^2, q_{j-1}^2\right).$$

If it is the emitted gluon that retains the characteristics we get an approximate emission probability

$$\frac{3\alpha_s}{\pi}\frac{dz_i}{z_i}\frac{dq_i^2}{q_i^2}\theta\left(q_i - q_{i-1}\right).$$

We now assume that $x$ is small and $Q^2$ large. For small $x$, we must have small $z_i$, in which case the latter of the possible gluon emission is the dominant one. And thus we have

$$G\big(x, Q^2\big) \approx \sum_{n=0}^{\infty}\left[\prod_{j=1}^{n}\int_{q_{j-1}^2}^{Q^2} dq_j^2 \int_{x/x_0}^{1} dz_j \left(\delta\left(x - x_0\prod_{j=1}^{n} z_j\right)\theta\left(Q^2 - q_n\right)\frac{3\alpha_s}{\pi q_j^2 z_j}\right)\right]$$

If we make the change of variables $x_i = \prod_{j=1}^{i} z_j$ and assume $x_0 = 1$ then

$$\ln(1/x_1) < \ln(1/x_2) < \ldots < \ln(1/x)$$

so there is an order, and

$$\left|\frac{d(x_1, \ldots, x_n)}{d(z_1, \ldots, z_n)}\right| = z_1^n z_2^{n-1}\cdots z_{n-1},$$

so that $\prod_{i=1}^{n}\frac{dz_i}{z_i} = \prod_{i=1}^{n}\frac{dx_i}{x_i}$. We make another change of variables, $l_i = \ln\left(1/x_i\right)$ and $\kappa_i = \ln\left(q_i^2\right)$, and we get that

$$\begin{aligned} G\big(x, Q^2\big) &\approx \sum_{n=0}^{\infty}\left[\prod_{j=1}^{n}\frac{3\alpha_s}{\pi}\int_{\kappa_{j-1}}^{\ln\left(Q^2\right)} d\kappa_j \int_{l_{j-1}}^{\ln(1/x)} dl_j\right] \\ &= \sum_{n=0}^{\infty}\left[\left(\frac{3\alpha_s}{\pi}\right)^n \frac{\left(\ln\left(Q^2\right)\right)^n}{n!}\frac{\left(\ln\left(1/x\right)\right)^n}{n!}\right] \end{aligned}$$

In the BFKL-equation it is assumed that both $x$ and $Q^2$ are small, but $Q^2$ is still large enough to use pQCD. For the gluon chains in this region there is no order for the transverse momentum of the emitted gluons. Instead we look at the propagator of the ladder gluon, $k_i^2$. In the DGLAP-region there is almost no difference between $q$ and $k$, but in BFKL there is a real distinction and the variable to look at in a chain is $k$. The space available to $k$ is small since $Q^2$ is small. Thus while emission where $k_i^2 > k_{i+1}^2$ are not forbidden they are suppressed by a factor $\frac{k_{i+1}^2}{k_i^2} = e^{-(\kappa_i - \kappa_{i+1})}$ where $\kappa = \ln\left(k\right)$. Thus we allow emissions where $\Delta\kappa < 1$, since this corresponds to a suppression factor less than $1/e$. One finds that the gluon function is

$$G(Y, \kappa) \approx e^{\frac{e3\alpha_s}{\pi}Y}.$$

Thus the number of soft gluon increases exponentially in $Y$. Thus it is enough to study the gluons if we are interested in the region were both $x$ and $Q^2$ are small, since they contribute to most of the momentum in this region.

Using the BFKL-equation, [13], one will instead get that

$$G(Y, \kappa) \approx e^{\frac{4\ln(2)3\alpha_s}{\pi}Y}$$

The increase is in fact larger than what is observed in experiments. In the derivation of the BFKL-equation one only uses the leading order terms. Thus there are large next to leading order corrections. This is related to saturation i.e. the cross section does not increase as fast after a certain energy is reached. As the number of gluons increase they interact with each other and start to recombine and reach a state of equilibrium between the emission and recombination processes.

## 1.3 Dipole formalism

Mueller developed a dipole formalism in coordinate space, [21, 22, 23], and showed that it was equivalent to the BFKL-equation. It is however possible to include non-linear behavior in the dipole model. The model describes gluons as being connected in dipoles with the end point gluons given in coordinate space. Fourier transforms makes it possible to go from coordinate space to momentum space.

In the dipole model the gluons does not emit independently, therefore, we get interference between nearby gluons.

We will use some classical arguments from electrodymanics to calculate the dipole splitting probability and the interaction probability for dipoles. These quantities have been calculated within pQCD, for calculations see [13] page 233 for the first quantity and [24] page 262 for the second.

We assume that we have two incoming protons with dipoles $\{d_i\}_{i=1}^{N}$ and $\{d_j\}_{j=1}^{M}$, respectively. For a single pair of dipoles, we denote the scattering amplitude squared by $f_{ij} = f(d_i, d_j)$. The amplitude is in some sense the average number of interactions that take place. If we assume that the interactions are independent,given by a Poisson distribution, the probability that there is no interaction is given by $e^{-f_{ij}}$. Thus the probability that no interactions at all takes place is $\prod_{ij} e^{-f_{ij}} = e^{-\sum_{ij} f_{ij}}$. Conversely the probability that at least one interaction takes place is

$$1 - e^{-\sum_{ij} f_{ij}}.$$

The emission process starts with a proton at rest. Since we do not know what an incoming proton wave function looks like, we will use a very simple model where the three valence quarks are replaced by three gluons connected in a equilateral triangle by three dipoles.

### 1.3.1 Emission

As the proton energy increase, the dipoles will radiate gluons. Consider a dipole, as in [18], with a charge at $\mathbf{x}_1$, and an anti-charge at, $\mathbf{x}_2$ moving rapidly in the $z$-direction. The color field measured by a stationary observer in a point, $\mathbf{r}$, is

$$E^2(\mathbf{r}) \propto \alpha_s \left| \frac{\mathbf{r}_1}{r_1^2} - \frac{\mathbf{r}_2}{r_2^2} \right|^2 = \alpha_s \frac{R^2}{r_1^2 r_2^2}$$

where $R = |\mathbf{r}_1 - \mathbf{r}_2|$ is the size of the dipole and $\mathbf{r}_i = \mathbf{x}_i - \mathbf{r}$ for $i = 1, 2$. Thus we have an energy intensity

$$I(t) \propto \alpha_s \frac{R^2}{r_1^2 r_2^2} \delta(t)\,,$$

and the number density of gluons is given by

$$\frac{dn}{dY} \propto \alpha_s \frac{R^2}{r_1^2 r_2^2} d^2\mathbf{r},$$

where $Y = \ln(1/x)$. A more rigorous calculation gives that the emission probability is

$$\frac{dP}{dy} = \frac{3\alpha_s}{2\pi^2}\frac{R^2}{r_1^2 r_2^2}d^2\mathbf{r},$$

where we have set $dY = dy$. It is possible to set $dY = dy$, since, if $x$ is the fraction of the protons positive LC-momentum carried by a gluon, i.e. $p_+ = xP_+$, then

$$y = \frac{1}{2}\ln\left(\frac{p_-}{p_+}\right) = \ln\left(\frac{p}{p_+}\right) = \ln\left(\frac{p}{xP_+}\right) = \ln(1/x) + \ln\left(\frac{p}{P_+}\right),$$

so that $dY = dy$.

The probability for emitting a dipole diverges when the gluon is emitted close to one of the parents, i.e. when one of the new dipoles is very small. As we will see below, small dipole have a very low interaction probability and therefore these small dipoles will not contribute to the cross section, and will be considered virtual fluctuations. Thus we may introduce a small cutoff for the minimum size of dipoles, and that removes the divergens.

The protons are accelerated by emitting gluons with increasing rapidity. The rapidity range is related to the CM-energy and mass of the accelerated protons. At rest we have that $P_+ = P_- = M$ and thus $y = 0$. At all times we have that

$$P_+P_- = E^2 - P_z^2 = M^2 + \left|\bar{P}\right|^2 - P_z^2 = M^2 + P^2 = M^2$$

if $P = 0$, which we assume since the proton move in the $z$-direction. Also, if the proton is relativistic then we have $P_+ \approx \sqrt{s}$. Thus

$$P_+/P_- = P_+^2/M^2 \approx s/M^2$$

for a proton moving at relativistic speeds in the $z$-direction. From this we can see that the minimum rapidity is $y = \frac{1}{2}\ln\left(M^2/s\right) \approx -\frac{1}{2}\ln\left(s/M^2\right)$ and the maximum rapidity is $y = 0$.

### 1.3.2 Interaction

To describe the interaction probability for dipoles we first find the potential for a color charge at $\mathbf{r}_1$. As we know that the color field, in a point $\mathbf{r}$, for this charge is $\mathbf{E}(\mathbf{r}) \propto \alpha_s \frac{\mathbf{r}-\mathbf{r}_1}{(\mathbf{r}-\mathbf{r}_1)^2}$, we must have a potential

$$V(\mathbf{r}) \propto \alpha_s \ln\left(\frac{|\mathbf{r}-\mathbf{r}_1|}{r_0}\right),$$

where $r_0$ is some constant that sets the zero-level of the potential. For a charge and an anti-charge in a dipole $d_i = (\mathbf{r}_{i1}, \mathbf{r}_{i2})$ the potential is

$$V(\mathbf{r}) \propto \alpha_s \ln(|\mathbf{r}-\mathbf{r}_{i1}|/r_0) - \alpha_s \ln(|\mathbf{r}-\mathbf{r}_{i2}|/r_0) = \alpha_s \ln\left(\frac{|\mathbf{r}-\mathbf{r}_{i1}|}{|\mathbf{r}-\mathbf{r}_{i2}|}\right).$$

For a particle with incoming momentum $\bar{k}_1$ and outgoing momentum $\bar{k}_1'$ we have a momentum transfer $\bar{q}_1 = \bar{k}_1' - \bar{k}_1$. The scattering amplitude in momentum-space is given by

$$f(\bar{q}_1) = \int e^{i\bar{q}_1\cdot\bar{r}} V(\bar{r})\, d^3\bar{r},$$

according to the Born approximation. For our collisions we assume that $q_{1z} = 0$, so the Fourier transform is two dimensional, and the momentum transfer is transversal. For two particles with momentum transfer, $\mathbf{q}_1$, $\mathbf{q}_2$, respectively, in the scattering, the scattering amplitude in momentum-space will be, $f(\mathbf{q}_1) \pm f(\mathbf{q}_2)$. So for an incoming dipole, $d_j = (\mathbf{r}_{j1}, \mathbf{r}_{j2})$, will have momentum-space scattering amplitude squared $(f(\mathbf{q}_{j1}) - f(\mathbf{q}_{j2}))^2$, which gives us a coordinate-space scattering amplitude squared

$$f_{ij} = f(d_i, d_j) = (V(\mathbf{r}_{j1}) - V(\mathbf{r}_{j2}))^2 \propto \alpha_s^2 \left( \ln\left( \frac{|\mathbf{r}_{j1} - \mathbf{r}_{i1}|}{|\mathbf{r}_{j1} - \mathbf{r}_{i2}|} \frac{|\mathbf{r}_{j2} - \mathbf{r}_{i2}|}{|\mathbf{r}_{j2} - \mathbf{r}_{i1}|} \right) \right)^2 .$$

Here we see that for a small dipole, $d_i$, $\mathbf{r}_{i1} \approx \mathbf{r}_{i2}$ and therefore $f_{ij} \approx 0$. A rigorous calculation would give a factor $\frac{\alpha_s^2}{2}$ instead of $\alpha_s^2$.

## 1.4 A modified dipole model

There are certain modification made to the Mueller dipole model in DIPSY. Among these are energy conservation, the dipole swing, confinement and a way to keep track of the transverse momentum of the gluons.

### 1.4.1 Energy conservation

In the evolution of a dipole state the probability for emission tends to infinity as the distance tends to zero. To stop this we introduce a cutoff that removes to small dipoles, in DIPSY this cutoff is dynamical. Small dipoles corresponds to large transverse momenta by $\mathbf{p} = \frac{\mathbf{r}}{r^2}$, as we motivate in the appendix. Thus, a too small dipole will have momentum that exceeds the CM-energy. The dynamical cutoff in DIPSY determines the minimum size of the new dipoles depending on the rapidity of the new gluon.

The energy conservation also determine which interactions are allowed, a collision between two dipoles is only allowed if the are enough $p_\pm$ in the left/right state to cover the needed $p_\mp$ in the right/left state to put the four gluons involved in the interaction on shell.

### 1.4.2 Dipole swing

In order for an MC to make sense it must give the same result independent of the Lorentz-frame in which the collision is being studied. If we, say, collide in the CM-frame, there are a number of subscatterings. As we move in rapidity towards one of the protons being at rest it has fewer dipoles and there are fewer subscatterings. Thus, assuming continuity in the interacting dipoles, some of the dipoles in the proton that has been further accelerated must have combined into fewer dipoles. Thus we must allow for dipoles to recombine. This is accomplished by the so-called dipole swing. The swing is not a recombination as such, but it allows the dipoles to reconnect. The swing probability for two dipoles, $d_i = (\mathbf{r}_{i1}, \mathbf{r}_{i2})$, $d_j = (\mathbf{r}_{j1}, \mathbf{r}_{j2})$, two swing into $d_i' = (\mathbf{r}_{i1}, \mathbf{r}_{j1})$ and $d_j' = (\mathbf{r}_{i2}, \mathbf{r}_{j2})$ is given by

$$\frac{\Delta P}{\Delta y} = \lambda \frac{(\mathbf{r}_{i1} - \mathbf{r}_{i2})^2 (\mathbf{r}_{j1} - \mathbf{r}_{j2})^2}{(\mathbf{r}_{i1} - \mathbf{r}_{j1})^2 (\mathbf{r}_{i2} - \mathbf{r}_{j2})^2}.$$

The coefficient $\lambda$ is chosen in such a way that we get enough swings without getting so many that the program is seriously slowed down, $\lambda = 1$ seems to work fine, and a larger value does not change the results. The is also an implicit factor $1/N_c^2$ which has to do with the fact that only dipoles of matching color are allowed to swing.

The dipole swing will give us saturation since the swing on average lowers the size of the dipoles. As we know, smaller dipoles have a lower interaction probability. Therefore, even if there are more dipoles in the relativistic proton in the rest frame of the other proton, fewer of them will interact, and most of the dipoles will be considered purely virtual fluctuations.

### 1.4.3 Confinement

It is a well known fact that the color force vanishes at large distances, about the size of a proton. This is due to the fact that there are no free color charges. All color charges are confined to color singlet objects like hadrons. The derivation of confinement follows [7] page 202.

We write the interaction probability as

$$f_{ij} = \frac{\alpha_s^2}{2}\big(\ln(|\mathbf{r}_{j1} - \mathbf{r}_{i1}|) - \ln(|\mathbf{r}_{j1} - \mathbf{r}_{i2}|) + \ln(|\mathbf{r}_{j2} - \mathbf{r}_{i2}|) - \ln(|\mathbf{r}_{j2} - \mathbf{r}_{i1}|)\big)^2,$$

and notice that

$$\frac{1}{2\pi}\ln(1/r) = \frac{1}{(2\pi)^2}\int \frac{e^{i\mathbf{k}\cdot\mathbf{r}}}{\mathbf{k}^2}.$$

To get the confinement, we exchange the Coulomb propagator for a Yukawa propagator i.e.

$$\frac{1}{\mathbf{k}^2} \to \frac{1}{\mathbf{k}^2 + M^2},$$

where $M = 1/r_{max}$. Then $\frac{1}{2\pi}\ln(1/r)$ goes to $\frac{1}{2\pi}K_0(r/r_{max})$. And we find that

$$f_{ij} = \frac{\alpha_s^2}{2}\left(K_0\left(\frac{|\mathbf{r}_{j1} - \mathbf{r}_{i1}|}{r_{max}}\right) - K_0\left(\frac{|\mathbf{r}_{j1} - \mathbf{r}_{i2}|}{r_{max}}\right) + K_0\left(\frac{|\mathbf{r}_{j2} - \mathbf{r}_{i2}|}{r_{max}}\right) - K_0\left(\frac{|\mathbf{r}_{j2} - \mathbf{r}_{i1}|}{r_{max}}\right)\right)^2.$$

In the limit, $r << r_{max}$, we have

$$K_0(r/r_{max}) \approx -\ln(r/r_{max})$$

and in the limit, $r >> r_{max}$, we have

$$K_0(r/r_{max}) \approx \frac{r_{max}}{r}e^{-r/r_{max}}.$$

Thus the different methods agree when $r$ is small, while the interaction probability decreases exponentially for large distances.

The emission probability is originally given by

$$\frac{dP}{dy} = \frac{3\alpha_s}{2\pi^2}\left(\frac{\mathbf{x}-\mathbf{z}}{(\mathbf{x}-\mathbf{z})^2} - \frac{\mathbf{y}-\mathbf{z}}{(\mathbf{y}-\mathbf{z})^2}\right)^2,$$

where $\mathbf{x}, \mathbf{y}, \mathbf{z}$ are the transverse coordinates for the parent gluons and the emitted gluon, respectively. As we know $\nabla\ln(r) = \frac{\mathbf{r}}{r^2}$, we let

$$\frac{\mathbf{r}}{r^2} = -\nabla\ln(1/r) \to -\nabla K_0(r/r_{max}) = \frac{\mathbf{r}}{r \cdot r_{max}}K_1(r/r_{max}).$$

In this case we get the following asymptotic behavior in the limits $r << R_{max}$ and $r >> r_{max}$,

$$\frac{\mathbf{r}}{r \cdot r_{max}} K_1(r/r_{max}) \approx \frac{\mathbf{r}}{r \cdot r_{max}} \frac{r_{max}}{r} = \frac{\mathbf{r}}{r^2}$$
$$\frac{\mathbf{r}}{r \cdot r_{max}} K_1(r/r_{max}) \approx \frac{\mathbf{r}}{r \cdot r_{max}} \sqrt{\frac{\pi r_{max}}{r}} e^{-r/r_{max}}$$

So the emission falls of exponentially at large distance an behaves in a correct manner at small distances.

Empirically we know that the logarithmic interaction probability is not entirely accurate if we want $r = \frac{1}{p}$, [19]. It breaks down when the distance between the two dipoles is small. The problem is that the probability goes like $(\ln(r))^2 \, d^2\mathbf{r}$ for small distances, and not like $d^2\mathbf{r} = \frac{d^2\mathbf{p}}{p^4}$, which we would like since we have Rutherford scattering for large $p$. We therefore use an interaction probability given by

$$8\alpha_s^2 \sin^2\left(\frac{\mathbf{r} \cdot \mathbf{r}_1}{r^2}\right) \sin^2\left(\frac{\mathbf{r} \cdot \mathbf{r}_2}{r^2}\right)$$

where $\mathbf{r}$ is the vector between the midpoints of the two dipoles and $\mathbf{r}_1, \mathbf{r}_2$ the dipole vectors. The factor 8 is chosen so that the sinus-interaction and the logarithmic-interaction are equivalent on large distances. The sinus-interaction does not incorporate confinement.

# Chapter 2

# MC algorithm

How reliable the results of the study are, depends on how the MC works. Therefore, we will describe the important aspects of DIPSY, without going into programming details.

## 2.1 The initial proton

A proton consist to first approximation of three vales quarks, colored by $r$, $g$ and $b$. In DIPSY we only consider dipoles so at the $b$ vertex we add a $\bar{g}$ at $g$ a $\bar{r}$ and at $r$ a $\bar{b}$. The dipoles are placed in an equilateral triangle where the size of the triangle is determined by a Gaussian distribution, with mean value $R_0$ and variance $R$. This model been tested in [7] and gives a good description for a proton. Cross sections and transverse momenta are dependent on $R_0$. Setting $R_0 \approx 3$ GeV$^{-1}$ and $R \approx 0.1$ GeV$^{-1}$ will give a good fit to experiments. We also set $\Lambda_{QCD} = 0.28$ GeV and $r_{max} = 3.5$ GeV$^{-1}$. Here $r_{max}$ is the confinement scale and $\Lambda_{QCD}$ is the energy where would $\alpha_s$ become infinite (this is avoided by freezing $\alpha_s$ below $\frac{1}{r_{max}}$).

## 2.2 Acceleration of initial state

The protons are accelerated over a rapidity range from $-\ln\left(\frac{s}{M^2}\right)$ to 0 by the emission of gluons. The process steps forward in rapidity, and in each step either an emission or swings is performed according to the following algorithm:

After $n$ steps we set $y_{min} = \sum_{i=1}^{n} \Delta Y_i$, where $\Delta Y_i$ are the rapidity steps in the previous steps. For each dipole we calculate the probability for its first emission. This is done by including a Sudakov factor that gives the probability that nothing has happened before the gluon emission. Thus for each dipole, we get an distribution for when it emits its first gluon

$$\frac{dP_{emit}}{d\Delta Y_i} e^{-\int_{y_{min}}^{y_{min}+\Delta Y_i} \frac{dP_{emit}}{dY} dY}.$$

We also calculate the probability for a first swing for each pair of color compatible dipoles, in a similar way. The fact that only color compatible dipoles are allowed to swing induces a factor $1/N_c^2$ in the swing probability. For each of these distributions we generate a $\Delta Y_i$, and we say that the one giving the lowest $\Delta Y_i$ happens first, unless $y_{min} + \Delta Y_i > 0$, in which case the emission process is complete.

If it is a swing that has the lowest $\Delta Y_i$ then the dipoles reconnect. Otherwise, the lowest $\Delta Y_i$ corresponds to a dipole $d = (\mathbf{r}_1, \mathbf{r}_2)$, emitting gluon with rapidity $y_3 = y_{min} + \Delta Y_i$. $\Delta Y_i$ is used to calculate the dynamical cutoff $\rho$, that is used to speed up the program. The coordinate $\mathbf{r}_3$ for the emitted gluon is generated in such a way that

$$|\mathbf{r}_3 - \mathbf{r}_1|, |\mathbf{r}_3 - \mathbf{r}_2| > \rho.$$

The transverse momentum of the new gluon is given by

$$\mathbf{p}_3 = \frac{\mathbf{r}_3 - \mathbf{r}_1}{(\mathbf{r}_3 - \mathbf{r}_1)^2} + \frac{\mathbf{r}_3 - \mathbf{r}_2}{(\mathbf{r}_3 - \mathbf{r}_2)^2}.$$

From this the positive LC-momentum is given by

$$p_{3+} = e^{-y_3} p_3.$$

Recoils are given to the parent gluons which will get new momenta

$$p'_{i+} = p_{i+} - \frac{|\mathbf{r}_i - \mathbf{r}_3|^2}{|\mathbf{r}_1 - \mathbf{r}_3|^2 + |\mathbf{r}_2 - \mathbf{r}_3|^2} p_{3+}$$

and

$$\mathbf{p}'_i = \mathbf{p}_i - \frac{\mathbf{r}_3 - \mathbf{r}_i}{(\mathbf{r}_3 - \mathbf{r}_i)^2}$$

for $i = 1, 2$. This will conserve $p_+$ and $\mathbf{p}$. We set $y'_i = \ln\left(\frac{p'_{i+}}{p'_i}\right)$ and $p'_{i-}$ such that the four momentum squared is zero, and is interpreted as the $p_-$ needed to put the partons on-shell. Now we demand that

$$\begin{aligned} p'_{1+},\, p'_{2+} &> 0 \\ p_{3-} &> p'_{1-},\, p'_{2-} \\ y_3 &> y'_1,\, y'_2. \end{aligned}$$

Emissions which do not fulfill these conditions are vetoed. After a swing or an emission some of the $\Delta Y_i$ may have to be recalculated, before the next step can be constructed.

## 2.3 The collision

All dipoles in the left-moving and all dipoles in the right-moving are combined in a list of possible dipole-dipole pairs with corresponding interaction probability. By possible me mean that there must be enough $p_\pm$ to put the four gluons on-shell. This is done by computing $f_{ij}$ for all pairs and setting $f_{ij} = 0$ if there is not enough $p_\pm$. The dipoles that may interact are then chosen at random, with at least one dipole pair chosen. The chosen dipole pairs are ordered by recoil, $p_{rec}$, where

$$\mathbf{p}_{rec} = \frac{(\mathbf{r}_{i1} + \mathbf{r}_{i2})/2 - (\mathbf{r}_{j1} + \mathbf{r}_{j2})/2}{|(\mathbf{r}_{i1} + \mathbf{r}_{i2})/2 - (\mathbf{r}_{j1} + \mathbf{r}_{j2})/2|^2},$$

and $\mathbf{r}_{kl}$ is the position of gluon, $l = 1, 2$, in dipole $k = i, j$. In the process a dipole may be chosen several times. Since we only want a dipole to interact once, we use the recoil order. We start at the highest recoil and remove those dipole pairs where one of the dipoles has already interacted. The dipole pair that gives the highest recoil will always happen.

At this stage all ancestors of the gluons of the interacting dipoles are considered to be real. All other gluons are considered virtual and are removed with their momentum divided among its neighbors. Also we remove some small dipoles that have been emitted with a too large probability.

# Chapter 3

# Results and Conclusions

Our results are divided into three sections, multiple interaction, correlation between $\langle 1/r \rangle$ and other variables and finally correlations between the number of scatterings and the number of charged particles. All results are at the Tevatron energy, 2000 GeV.

## 3.1 Multiple interactions

In this section we study the distribution of the number of subscatterings, both at fixed impact parameter and average over all impact parameters. We will also study the impact parameter profile which gives the correlation between the number of subscatterings and the impact parameter.

### 3.1.1 Distributions

#### Results

In Figure 3.1 we show the distribution of the number of subscatterings at some given impact parameters. The distributions are compared to Poisson and geometric distributions. At low impact parameters, $b < 5$ GeV$^{-1}$, the distribution of the number of subscatterings is consistent with a Poisson distribution, while at large impact parameters, $b > 10$ GeV$^{-1}$, it behaves more like a geometric distribution.

Figure 3.2 shows the distribution of the number of subscatterings integrated over all impact parameters. The integrated distribution behaves like a geometric distribution for low numbers of subscattering, $N_{scatt} < 7$. For $N_{scatt} > 7$ there are deviations from the geometric distribution but it is still far from a Poisson. The average number of subscatterings over all impact parameters is $\langle N_{scatt} \rangle$ 1.97.

#### Conclusions

The shape of the distribution seems to indicate that DIPSY provides us with a dynamical explanation for the assumption of a Poisson distribution in PYTHIA. The distributions do not fit exactly, but, there is no theoretical reason why the distributions should be Poisson. Also, at large impact parameters the difference between geometric and Poisson distributions is very small.

The distribution integrated over all impact parameters also provides us with a dynamical explanation for the assumptions in PYTHIA, as we know, [14], that the

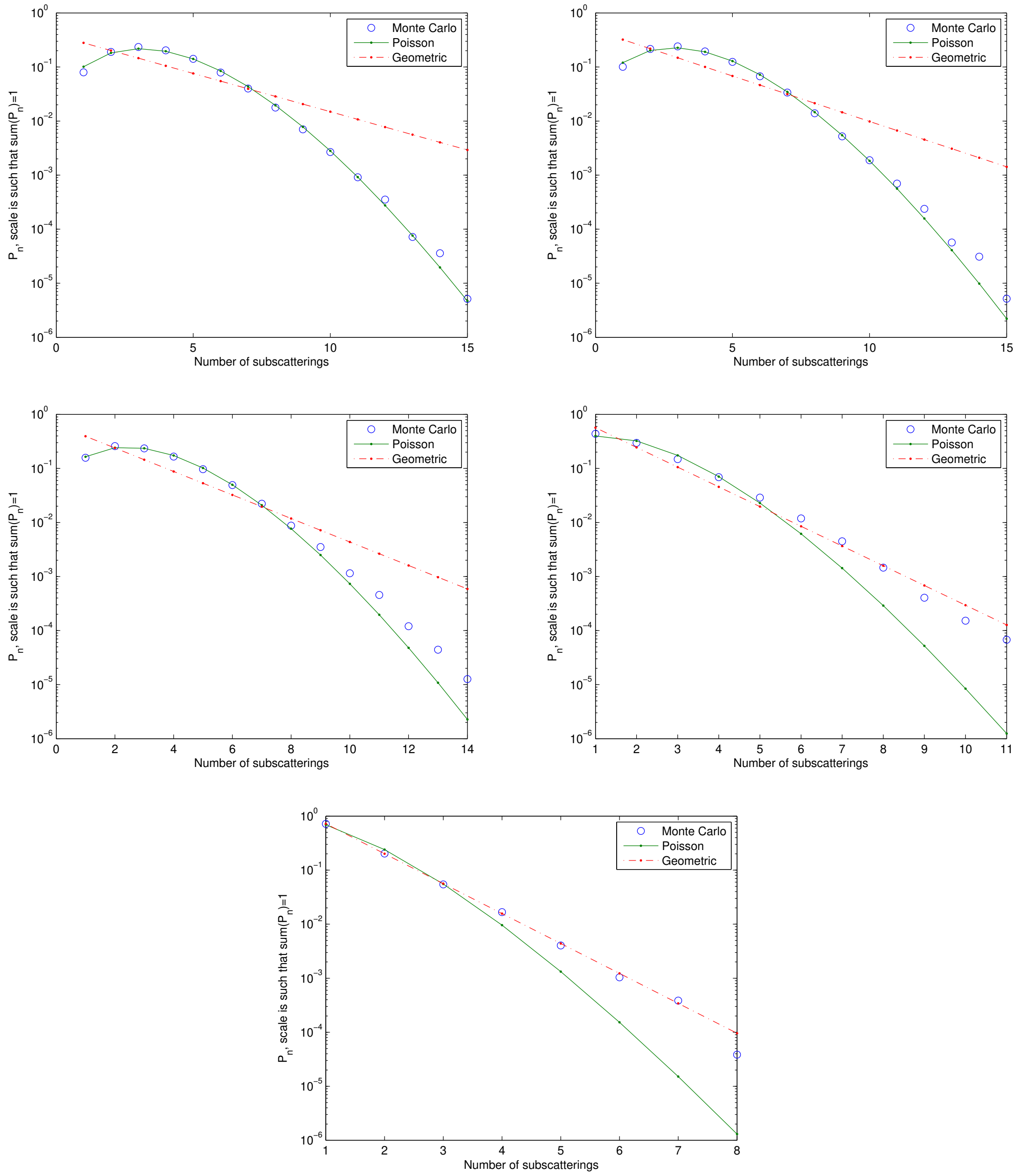


Figure 3.1: The number of subscatterings at impact parameters $b = 0, 1, 2, 5, 10$ GeV$^{-1}$. Notice that the $y$-axis is given in log-scale.

double Gaussian gives approximately a geometric distribution. It is the fact that we have a distribution that is wider than a Poisson, that is the reason why we must replace $\sigma_{tot}$ by something smaller in

$$\sigma_2 = \frac{1}{2}\frac{\sigma_1^2}{\sigma_{tot}}.$$

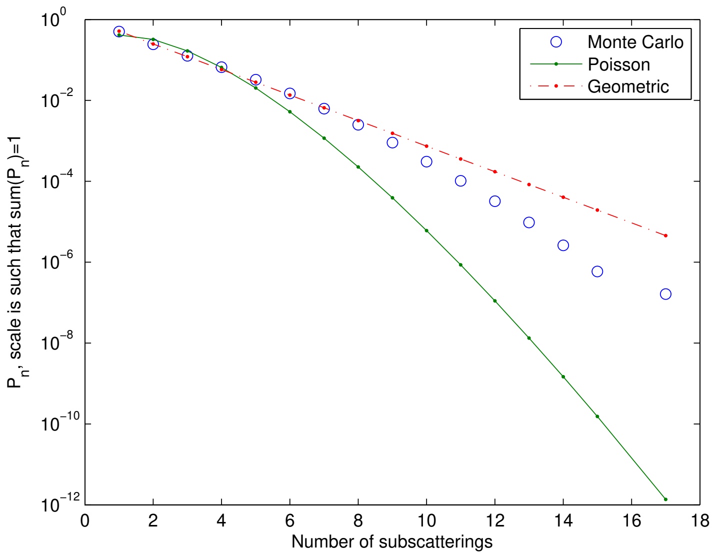


Figure 3.2: The number of subscatterings integrated over all impact parameters. Notice that the $y$-axis is given in log-scale.

### 3.1.2 Impact parameter profile

**Results**

To the left in Figure 3.3 we show the logarithm of the impact parameter profile. To the right we show the difference between the data and an exponential regression of the logarithm of the impact parameter. We see that $\ln(\langle N_{scatt}(b)\rangle_{all\,ev})$ has a

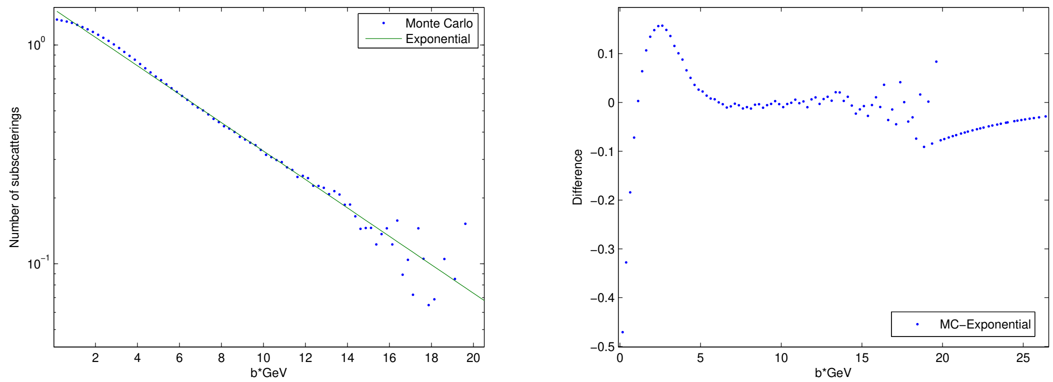


Figure 3.3: Impact parameter profile and the difference to the exponential. Notice that the $y$-axis is given in log-scale in the left figure.

exponential behavior at large impact parameters. At low impact parameters there is however a higher probability for interaction than the one given by the exponential. This becomes smaller than the exponential at very small impact parameters.

#### Conclusions

That our impact parameter profile has a bump for small $b$ seems to agree with the double Gaussian in PYTHIA, even if we do not get exactly the same form, the overall behavior that the density increases more in the middle, is reproduced. The impact parameter profile is more peaked in the middle than a exponential or a gaussian.

## 3.2 Correlations between $\langle 1/r \rangle$ and other variables

### 3.2.1 Correlation between $N_{dips}$ and $\langle 1/r \rangle$

The screening is related to the distance where the color field of a parton vanishes which in turn is related to the sizes of the dipoles.

#### Results

In Figure 3.4 we see how the initial proton evolves. We start with three equal dipoles with length $R_0$. These then split into more dipoles. We look at the distribution of the dipole sizes after the evolution. We look separately at the evolutions that end up with less than 40 dipoles, the evolutions that end with more than 40 dipoles, and the average case. We find that the number of large dipoles is larger in the case were

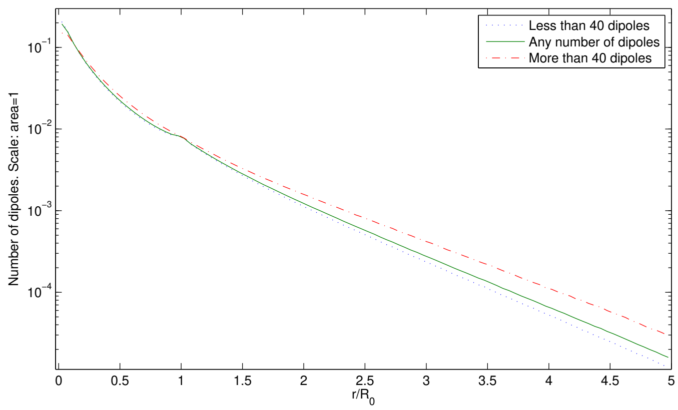


Figure 3.4: Evolution of the initial dipole.

we end up with more than 40 dipoles than in the other cases. The curve for more than 40 dipoles lies above the others for $r > 0.2R_0$, for $r$ less it drops below these.

In Figure 3.5 we show the behavior of $\langle\langle 1/r \rangle_{ev}\rangle_{all\,ev}$, i.e the average inverse size in an event averaged over all events, as a function of the number of dipoles in the colliding states. To the left we have the number of dipoles before the collision and to the right the number of dipoles after the collision. The curves named, "Weight of data", give a measure of the significance of the data for a particular number of dipoles. We see that before the collision the average inverse size of the dipoles decrease as a function of the number of dipoles, $\langle\langle 1/r \rangle_{ev}\rangle_{all\,ev}\, \langle 1/r \rangle \propto 1/N_{dips}^{0.692}$, and $\langle\langle 1/r \rangle_{ev}\rangle_{all\,ev} \approx 6$ GeV. However, after the collision the average inverse size of the dipoles increase, $\langle\langle 1/r \rangle_{ev}\rangle_{all\,ev} \propto N_{dips}^{0.527}$, and we have $\langle\langle 1/r \rangle_{ev}\rangle_{all\,ev} \approx 0.6$ GeV.

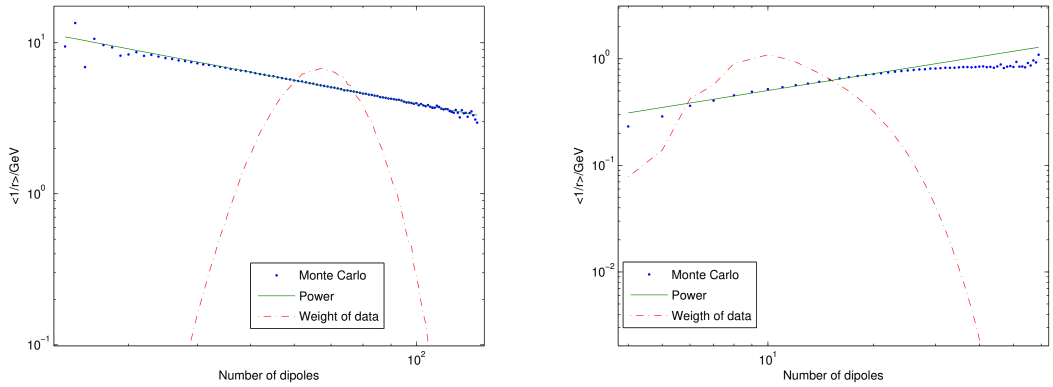


Figure 3.5: Average inverse dipole size as a function of the number of dipoles before and after the collision. Notice that both axes are in log-scale.

**Conclusions**

In the evolution of the initial state we see that there are fewer small dipoles created and more large created when there are a lot of dipoles created. This tells us that the energy conservation is strong. While the emission process favors small dipoles the energy conservation does not, since small dipoles correspond to large transverse momenta, which require a lot of energy.

In Figure 3.5, we see that the removal of small dipoles is more efficient when there are more dipoles. Since we go from a decreasing function to an increasing function, for $\langle\langle 1/r\rangle_{ev}\rangle_{all\,ev}$ in the collision.

### 3.2.2 Correlation between $N_{scatt}$ and $\langle 1/r\rangle$

**Results**

In Figure 3.6 we see $\langle\langle 1/r\rangle_{ev}\rangle_{all\,ev}$ as a function of the number of scatterings to left, and to the right we show the distribution of $\langle 1/r\rangle_{ev}$ for different number of scatterings. The right figure is scaled so that the area is 1. We get decreasing dipole

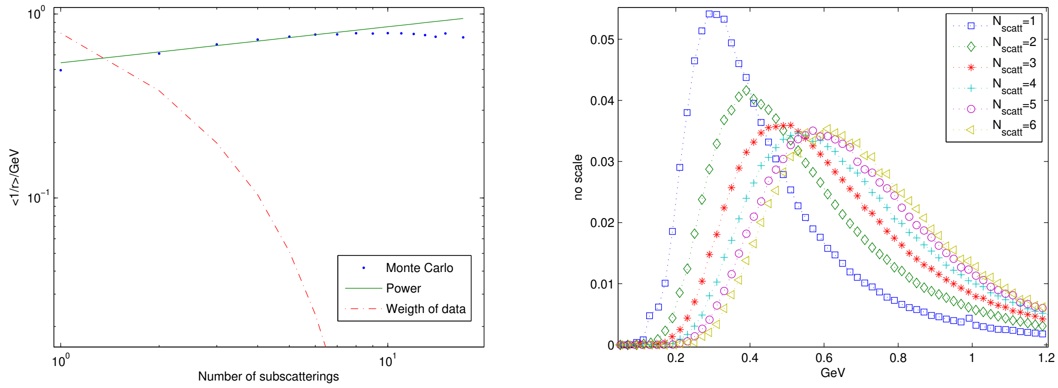


Figure 3.6: Average inverse dipole size by the number of scatterings after the collision. Notice that both axes are in log-scale in the left figure.

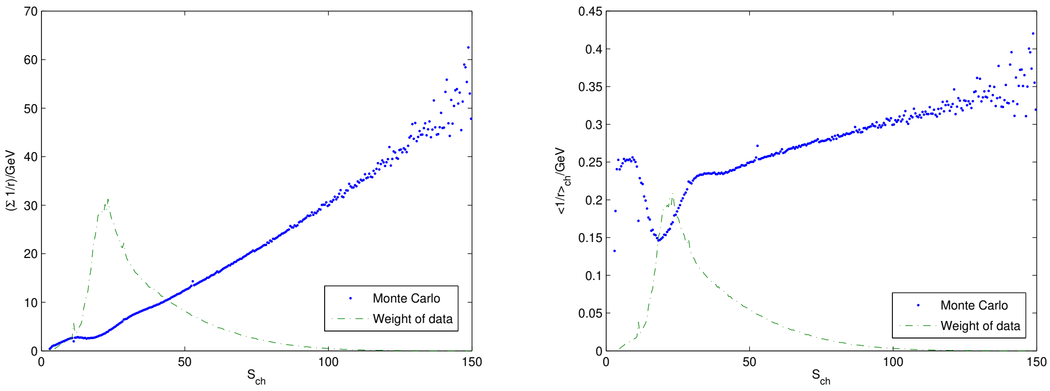


Figure 3.7: The sum of $\frac{1}{r}$ as a function of $S_{ch}$, and the sum divide by $S_{ch}$ as a function of $S_{ch}$.

sizes as the number of subscatterings increase, $\langle\langle 1/r\rangle_{ev}\rangle_{all\,ev} \propto N_{scatt}^{0.196}$. From the right figure we see that there is less variation in the inverse dipole sizes between the events if there are fewer subscatterings.

**Conclusions**

The increase in $\langle\langle 1/r\rangle_{ev}\rangle_{all\,ev}$ seen in Figure 3.6 is interesting compared to the results in [8]. It gives some evidence for enhanced screening. Assuming $\langle p\rangle \approx \langle 1/r\rangle$, we have found that the average transverse momentum increases with the number of subscattering.

### 3.2.3 Correlation between $N_{ch}$ and $\langle 1/r\rangle$

We make an attempt to calculate the charged multiplicity, $N_{ch}$, by using that the mass/energy of a string piece is

$$m^2 \approx \frac{1}{r^2}\left(e^{y_1}+e^{y_2}\right)\left(e^{-y_1}+e^{-y_2}\right),$$

where $r$ is the size of the dipole and $y_1$, $y_2$ are the rapidities of the two gluons at the endpoints. We will say that

$$S_{ch} = \sum_{j=1}^{N_{dips}} \ln(1+\frac{m_j^2}{m_0^2}),$$

where $m_0^2 = 0.5$ GeV$^2$ and $S_{ch} \propto N_{ch}$. We add a 1 in the logarithm to ensure that all string pieces give positive contributions.

**Results**

In Figure 3.7, we see $\left\langle \sum_{j=1}^{N_{dips}} \frac{1}{r_j} \right\rangle_{all\,ev}$, as a function of $S_{ch}$, to the left, and $\left\langle \sum_{j=1}^{N_{dips}} \frac{1}{r_j} \right\rangle_{all\,ev} / S_{ch}$ as a function of $S_{ch}$, to the right.

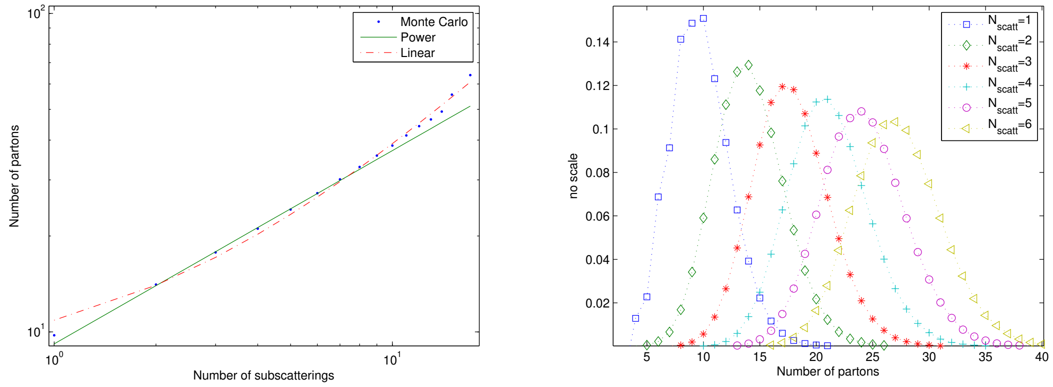


Figure 3.8: The number of partons by number of subscatterings. Notice that both axes are in log-scale in the left figure.

#### Conclusions

We set

$$\langle p\rangle(S_{ch}) \approx \frac{c_0 S_{ch} + \left\langle \sum_{j=1}^{N_{dips}} \frac{1}{r_j} \right\rangle_{all\,ev} (S_{ch})}{S_{ch}},$$

where $c_0$ is the supposed to be the part that comes form the string breaking. Since $\left\langle \sum_{j=1}^{N_{part}} \frac{1}{r_j} \right\rangle_{all\,ev} (S_{ch})$ increases more than a linear function we get an increase in $\langle p\rangle$. The increase is seen in the right figure of Figure 3.7. This shows that DIPSY can explain some of the increase in $\langle p\rangle(S_{ch})$.

Our formula for $S_{ch}$ is probably wrong for small values since there is a peak there, which we do not expect.

## 3.3 Correlation between $N_{part}$ and $N_{scatt}$

#### Results

Figure 3.8 shows the relation between the number of real partons after the collision and the number of subscatterings. To the left we have $\langle N_{part}\rangle_{all\,ev}$, and to the right we have the distribution of $N_{part}$ for different $N_{scatt}$. For $N_{scatt} = 1, \ldots, 8$ the number of partons increases like a power, $\langle N_{part}\rangle_{all\,ev} \propto N_{scatt}^{0.607}$, but for $N_{scatt} > 7$ it increases linearly.

#### Conclusion

It is quite rare that there are more than 8 subscatterings, so the increase grows like a power. Now, since we in fact have $N_{part} = N_{dips}$, and we see that $N_{scatt}$ and $N_{part}$ highly correlated, it seems natural that $\langle\langle 1/r\rangle_{ev}\rangle_{all\,ev}$ is an increasing function of both $N_{scatt}$ and $N_{dips}$.

# Chapter 4

# Outlook

In this thesis we presented how multiple interactions is introduced in the standard parton model. We also presented a modified version of the Mueller dipole model that we hope will give dynamical method to get the same results as in the multiple interaction model. DIPSY gives gives convincing results when it comes to the impact parameter profile, and the distributions of the number of scatterings both a fixed impact parameter and averaged over all impact parameters.

As for the increase in $\langle p \rangle (N_{ch})$, that is seen in experiments, we only get indirect results. The correlation between $\langle 1/r \rangle$ and $N_{scatt}$ indicates an enhanced screening effect. The correlation between $\sum \frac{1}{r}$ and $N_{ch}$ also indicates that DIPSY gets an increase in $\langle p \rangle (N_{ch})$. To fully test this increase we need the exclusive final states with both position and momenta of the on-shell gluons created in the collision. To get there we will need a correspondence between the transverse momentum of a emitted gluon and the distance from its parent gluons, we will need a method for calculating the recoils to the gluons in an interaction. Finally, we must make sure that we remove all virtual fluctuations.

# Appendix

In the appendix we will calculate some of the formulas that are needed in this thesis.

## Electric field of a moving electron

A stationary electron will have an electric field $\bar{E} \propto \frac{\bar{r}}{|\bar{r}|^3}$. According to [20], page 559, the electric field of an electron moving at speed $v = \beta c$ in the $z$-direction, observed by a stationary observer at a point $X_\mu = (t, r_x, 0, 0)$, will be

$$\begin{aligned} E_x(t) &= \frac{e\gamma r_x}{\left(r_x^2 + (\gamma v t)^2\right)^{3/2}}, \\ E_y(t) &= 0, \\ E_z(t) &= -\frac{e\gamma v t}{\left(r_x^2 + (\gamma v t)^2\right)^{3/2}}, \end{aligned}$$

where $\gamma = \frac{1}{\sqrt{1-\beta^2}}$, and we assume that the electron is at $(t, 0, 0, vt)$. The magnetic field is given by

$$\begin{aligned} B_x(t) &= 0, \\ B_y(t) &= \beta E_x(t)\,, \\ B_z(t) &= 0. \end{aligned}$$

We see that the $x$-component of the field will behave as a spike at $t = 0$, if the particle is moving at nearly the speed of light. So we approximate the field by

$$\bar{E}(t) \approx \bar{E}_0 \delta(t)$$

where $\bar{E}_0 = \int_{-\infty}^{\infty} \bar{E}(t)\, dt$. Using $\int_{-\infty}^{\infty} \frac{1}{(x^2+a^2)^{3/2}} dx = \frac{2}{a^2}$ we obtain

$$\int_{-\infty}^{\infty} E_x(t)\, dt = \frac{e}{r_x v} \text{ and } \int_{-\infty}^{\infty} E_z(t)\, dt = 0.$$

By rotating around the $z$-axis we see that

$$\bar{E}_0 \propto \left(\frac{\mathbf{r}}{r^2}, 0\right).$$

## Fourier transforms

In $\mathbb{R}^2$ the function $f(\mathbf{x}) = \frac{1}{|x|^\alpha}$ can be Fourier transformed, [28], as a tempered distribution for $\alpha < 2$, with

$$\mathcal{F}\left(\frac{1}{|\mathbf{x}|^\alpha}\right) = \frac{\pi 2^{2-\alpha}\Gamma\left(1-\frac{\alpha}{2}\right)}{\Gamma\left(\frac{\alpha}{2}\right)}|\mathbf{p}|^{\alpha-2}.$$

It will, however, not be defined for $\alpha = 2$. We however need this since it corresponds to a Coulomb propagator. In order to be able to Fourier transform it we define the finite part distribution by

$$f.p.\frac{1}{p^2}(\phi) = \int_{p<1}\frac{\phi(\mathbf{p})-\phi(0)}{p^2} + \int_{p>1}\frac{\phi(\mathbf{p})}{p^2}.$$

This will be a well defined tempered distribution on $\mathbb{R}^2$ with

$$\mathcal{F}^{-1}\left(f.p.\frac{1}{p^2}\right) = \frac{1}{(2\pi)^2}\int\frac{e^{i\mathbf{r}\cdot\mathbf{p}}}{p^2} = \frac{1}{2\pi}\ln(1/r) + (\text{some constant}).$$

We also need the formula for the Yukawa potential. In $\mathbb{R}^n$ we define

$$G_\alpha(x) = \frac{1}{(2\pi)^n}\int\frac{e^{i\xi\cdot x}}{(1+|\xi|^2)^{\alpha/2}}d^n\xi,$$

it can be shown, see [1], that

$$G_\alpha(x) = c_\alpha\frac{1}{|x|^{(n-\alpha)/2}}K_{(n-\alpha)/2}(|x|)$$

where $1/c_\alpha = 2^{(\alpha-2)/2}(2\pi)^{n/2}\Gamma(n/2)$, and $K_\nu$ are modified Bessel functions of the third kind.

The asymptotic behavior for modified Bessel functions of the third kind are

$$\begin{aligned} K_0(r) &\approx \ln(1/r) \\ K_\nu(r) &\approx \frac{2^{\nu-1}\Gamma(\nu)}{r^\nu} \quad , \text{for } \nu > 0 \end{aligned}$$

in the limit $r \to 0$, and

$$K_\nu(r) \approx \left(\frac{\pi}{2r}\right)^{1/2} e^{-r}$$

in the limit $r \to \infty$.

## Relation between r and p

Supposing that the distribution in $\mathbf{r}$ is given by $\frac{dn}{d^2\mathbf{r}} = |\psi(\mathbf{r})|^2 = \frac{1}{r^2}$. Now since $\mathcal{F}\left(\frac{1}{|\mathbf{r}|}\right) = \frac{1}{|\mathbf{p}|}$, we get that

$$\phi(\mathbf{p}) = \int d^2\mathbf{r}\psi(\mathbf{r})\,e^{i\mathbf{r}\cdot\mathbf{p}} = \frac{2\pi}{p},$$

and $\frac{dn}{d^2\mathbf{p}} = |\phi(\mathbf{p})|^2 = \frac{1}{p^2}$. From this we get that $\frac{d^2\mathbf{r}}{r^2} = dn = \frac{d^2\mathbf{p}}{p^2}$. This correspondence also holds if we assume that $\mathbf{p} = \frac{\mathbf{r}}{r^2}$ or equivalently $\mathbf{r} = \frac{\mathbf{p}}{p^2}$. We have

$$\frac{dr_x}{dp_x} = \frac{p_y^2 - p_x^2}{\left(p_x^2 + p_y^2\right)^2} \text{ and } \frac{dr_x}{dp_x} = \frac{-2p_x p_y}{\left(p_x^2 + p_y^2\right)^2}$$

so that

$$\left|\frac{d(\mathbf{r})}{d(\mathbf{p})}\right| = \frac{1}{p^4} = \frac{r^2}{p^2}.$$

Thus we find that

$$\frac{d^2\mathbf{r}}{r^2} = \frac{d^2\mathbf{p}}{p^2}$$

and also

$$d^2\mathbf{r} = \frac{d^2\mathbf{p}}{p^4} \text{ and } \frac{d^2\mathbf{r}}{r^4} = d^2\mathbf{p}.$$

# Bibliography


[1] D. R. Adams, L. I. Hedberg, *Function spaces and potential theory*, Grundlehren der mathematischen Wissenschaften **314**, 1996.

[2] B. Andersson, G. Gustafson, G. Ingelman, T. Sjöstrand, *Parton Fragmentation and String Dynamics*, Phys. Rep. **97** (2-3), 31-145, (1983).

[3] B. Andersson, P. Dahlqvist, G. Gustafson *On local parton-hadron duality* , Z. Phys. C **44**, 455-460 (1989).

[4] E. Asvar, G. Gustafson, L. Lönnblad, *Energy Conservation and Saturation in Small-x Evolution*, JHEP **07**(062), (2005).

[5] E. Asvar, G. Gustafson, L. Lönnblad, *Small-x Dipole Evolution Beyond the Large-$N_c$ Limit*, JHEP **01**(012), (2007).

[6] E. Asvar, G. Gustafson, *Geometric Scaling and QCD Dynamics in DIS*, JHEP **04**(067), (2007).

[7] E. Asvar, G. Gustafson, L. Lönnblad, *Diffractive Excitation in DIS and pp Collisions*, JHEP **12**(012), (2007).

[8] R. Corke, *Multiple Interactions in Pythia 8*, arXiv, hep-ph/ 0901.2852, (2009).

[9] R.D. Fields *Min-Bias and the Underlying Event at the Tevatron and the LHC*, Fermilab ME/MC Tuning Workshop, October 4, 2002.

[10] C. Flensburg, G. Gustafson, L. Lönnblad, *Elastic and quasi-elastic pp and $\gamma^*p$ scattering in the Dipole Model*, Eur. Phys. J. **C60** (2), 233-247, (2009).

[11] C. Flensburg, *Quasielastic Scattering in the Dipole Model*, arXiv, hep-ph/ 0902.3606, (2009).

[12] C. Flensburg, L. Lönnblad, in preparation.

[13] J.R. Forshaw, D.A. Ross, *Quantum Chromodynamics and the Pomeron*, Cambrige lecture notes in physics **9**, CUP, 1997.

[14] G. Gustafson, L. Lönnblad, G. Miu, *Hadronic Collisions in the Linked Dipole Chain Model*, Phys. Rev. **D67**, (2003).

[15] G. Gustafson, *An Intuitive Semiclassical Picture of Proton Structure at Small $x$*, Acta Physica Polonica, **B34**, (2003).

[16] G. Gustafson, *Multiple Scattering, Underlying Event, and Minimum Bias*, arXiv, hep-ph/ 0712.1941, (2007).

[17] G. Gustafson, *The Lund Model, Multiple Scattering, and Final States*, Acta Physica Polonica, **B39**, (2008).

[18] G. Gustafson, *Multiple Interactions Saturation, and Final States in* **pp** *Collisions and DIS*, Conference paper, Epiphany Conference, January 2009.

[19] G. Gustafson, Private communication.

[20] J. Jackson, *Classical electrodynamics* 3 edition, Wiley, 1999.

[21] A.H. Mueller, *Soft gluons in the infinite-momentum wave function and the BFKL pomeron*, Nuclear Physics **B415**, 373-385, (1994).

[22] A.H. Mueller, B. Patel, *Single and double BFKL pomeron exchange ans a dipole picture of high energy hard processes*, Nuclear Physics **B425**, 471-488, (1995).

[23] A.H. Mueller, *Unitatity and the BFKL pomeron*, Nuclear Physics **B437**, 107-126, (1995).

[24] H. Navelet, S. Wallon, *Onium-onium scattering at fixed impact parameter: exact equivalence between the color dipole model and the BFKL pomeron*, Nuclear Physics **B522**, 237-281, (1998).

[25] G.P. Salam, *Studies of unitarity at small x using dipole formulation*, Nuclear Physics **B461**, 512-538 (1996).

[26] T. Sjöstrand, M. van Zijl, *A multiple-interaction model for the event structure in hadron collisions*, Phys. Rev. **D36**, (1987).

[27] T Sjöstrand, P.Skands, *Multiple Interactions and the Structure of Beam Remnants*, JHEP, **0403**, 053,(2004)

[28] R. Strichartz, *A Guide to Distribution theory and Fourier Transforms*, World Scientific, 2003.